Fundamental Research 5 (2025) 72–81

Contents lists available at ScienceDirect

Fundamental Research

journal homepage: http://www.keaipublishing.com/en/journals/fundamental-research/

Article

Multi-channel microelectrode arrays for detection of single-cell level neural information in the hippocampus CA1 under general anesthesia induced by low-dose isoflurane

Ruilin Hu[a,b], Penghui Fan[a,b], Yiding Wang[a,b], Jin Shan[a,b], Luyi Jing[a,b], Wei Xu[a,b], Fan Mo[a,b], Mixia Wang[a,b], Yan Luo[c], Ying Wang[c,*], Xinxia Cai[a,b,*], Jinping Luo[a,b,*]

[a] State Key Laboratory of Transducer Technology, Aerospace Information Research Institute, Chinese Academy of Science, Beijing 100190, China
[b] University of Chinese Academy of Sciences, Beijing 100049, China
[c] Department of Anesthesiology, Ruijin Hospital, Shanghai Jiao Tong University School of Medicine, Shanghai 200020, China

ARTICLE INFO

Article history:
Received 13 March 2023
Received in revised form 17 April 2023
Accepted 10 May 2023
Available online 19 June 2023

Keywords:
Micro electrode array
Hippocampal CA1
Isoflurane anesthesia
Spike
Local field potentials

ABSTRACT

Timely monitoring of anesthesia status during surgery is important to prevent an overdose of isoflurane anesthesia. Therefore, in-depth studies of the neural mechanisms of anesthetics are warranted. Hippocampal CA1 plays an important role during anesthesia. Currently, a high spatiotemporal resolution microdevice technology for the accurate detection of deep brain nuclei is lacking. In this research, four-shank 32-channel implantable microelectrode arrays (MEAs) were developed for the real-time recording of single-cell level neural information in rat hippocampal CA1. Platinum nanoparticles were modified onto the microelectrodes to substantially enhance the electrical properties of the microelectrode arrays. The modified MEAs exhibited low impedance (11.5 ± 1 kΩ) and small phase delay (-18.5° ± 2.54°), which enabled the MEAs to record single-cell level neural information with a high signal-to-noise ratio. The MEAs were implanted into the CA1 nuclei of the anesthetized rats, and the electrophysiological signals were recorded under different degrees of anesthesia mediated by low-dose concentrations of isoflurane. The recorded signals were analyzed in depth. Isoflurane caused an inhibition of spike firing rate in hippocampal CA1 neurons, while inducing low-frequency oscillations in CA1, thus enhancing the low-frequency power of local field potentials. In this manner, the spike firing rate and the power of local field potentials in CA1 could characterize the degree of isoflurane anesthesia. The present study provides a technical tool to study the neural mechanisms of isoflurane anesthesia and a research method for monitoring the depth of isoflurane anesthesia in clinical practice.

1. Introduction

Anesthesia is a controlled, temporary state of sensory or consciousness loss, which is often utilized for medical purposes such as surgery to prevent intraoperative perception in patients or laboratory animals, thereby reducing the perceived pain and creating good surgical conditions [1]. Isoflurane is an inhaled general anesthetic with the characteristics of rapid action, stable potency, controllability, and short recovery periods of anesthesia. Isoflurane is commonly used in animal surgery [2,3] and experiments in neuroscience [4]. However, numerous studies have reported that isoflurane alters the characteristics of cerebral tissue activity and affects the neural signals in the cerebrum [5,6], and an overdose of isoflurane can even result in death [7]. Therefore, it is critical to monitor the depth of isoflurane anesthesia during surgery in real time accurately.

Previous studies have demonstrated that the hippocampus in the brain participates in the anesthetic procedure of isoflurane, and the isoflurane-induced effects including the inhibition of glutamatergic excitatory postsynaptic potentials, enhancement of GABAergic inhibitory postsynaptic potentials, as well as suppression of excitatory transmission [8]. All of these exert an effect on the hippocampal electrophysiological signals [9], which is also widely believed to be responsible for anesthetic-induced amnesia [10,11]. Therefore, it is believed that hippocampal CA1 electrophysiological signals could characterize the depth of isoflurane anesthesia. A detailed study on the hippocampal CA1 electrophysiological signals under isoflurane anesthesia could reveal the neural mechanisms of general anesthesia and provide a research method for the clinical monitoring of the degree of anesthesia.

Currently, most studies on the mechanisms of anesthetics are focused on the following categories. One category is anatomy-based stud-

* Corresponding authors.
E-mail addresses: wy10879@rjh.com.cn (Y. Wang), xxcai@mail.ie.ac.cn (X. Cai), jpluo@mail.ie.ac.cn (J. Luo).

https://doi.org/10.1016/j.fmre.2023.05.015

ies on the neural mechanisms of isoflurane anesthesia, conducted at the molecular level [12–14], which are sensitive and selective, although they provide poor spatial and temporal resolution. Brain activity during the isoflurane anesthesia procedure may also be monitored using non-invasive means such as electroencephalogram (EEG) and functional magnetic resonance imaging, which could be directly applied clinically although challenges of complex data processing and poor spatial resolution are encountered [15–17]. The detection of local field potentials (LFPs) in the deep brain under isoflurane anesthesia using microfilament or tungsten wire electrodes [18], is another approach that provides improved spatiotemporal resolution, although it does not allow for recording the activity of individual neurons. Therefore, it is important to investigate the anesthetic mechanisms of isoflurane at the level of neuronal activity. In this context, implantable multi-channel microelectrode arrays (MEAs) with high spatiotemporal resolution that would provide real-time recording of single-cell level neural information in the deep brain become important [19–21]. In order to enhance the recording capability of MEAs, the surfaces of microelectrodes were modified with nanomaterials. As metallic nanoparticles, platinum nanoparticles (PtNPs) are used widely in medical, electronic and biotechnological applications due to their biocompatibility, high stability and surface chemistry properties [22]. The modification with PtNPs effectively increases the surface area of microelectrodes, thereby reducing the impedance of microelectrodes, improving the signal-to-noise ratio (SNR), and enhancing the detection capability of the MEAs.

In the present study, four-shank 32-channel MEAs were large-scale fabricated for real-time, high spatiotemporal resolution and multichannel detection of electrophysiological signals from rat hippocampal CA1. In addition, microelectrodes were modified with PtNPs to enhance their electrical properties. The MEAs were implanted into rat hippocampus CA1 to detect electrophysiological signals. The in vivo research has demonstrated that PtNPs-modified MEAs provide a steady and sensitive recording of the single-cell level neural information in rat hippocampal CA1. In addition, the dynamic change characteristics of electrophysiology deliver a method for the detection of the depth of isoflurane anesthesia.

2. Materials and methods

2.1. Materials and apparatus

The saline was purchased from Shuanghe Corporation (China). The phosphate-buffered saline (PBS) was purchased from Sigma-Aldrich (China). Chloroplatinic acid (H_2PtCl_6) and lead acetate [$(CH_3COO)2$ Pb] were purchased from Sinopharm Chemical Reagent (China). Isoflurane and the anesthesia machine for small animals were purchased from RWD Life Science Co. Ltd. (China).

The rats were fixed in the stereotaxic frame (51600, Stoelting, USA) for craniotomy. The MEAs were connected to the micropositioner (model 2662, David KOPF instrument, USA) to control the implantation depth of the MEAs. The surface of the microelectrode was observed using two microscopes (BX51, Olympus Corporation, Japan and M205C, Leica Biosystems, USA). The MEAs were modified and characterized using the electrochemical workstation (Gamry, USA). The head stages and the electrophysiological signal recording equipment were homemade, as previously reported [23,24], which were used for recording the electrophysiological signals detected by MEAs.

All animal experiments were conducted in accordance with the ethical animal welfare requirements of the Aerospace Information Research Institute, Chinese Academy of Science (Approval No. AIRCAS-006-2). All animals used in the experiments were fed separately in a professional biological laboratory, where the room temperature was controlled to be within the range of 22–25 ˚C, the relative humidity was maintained between 30% and 50%, a natural light-dark cycle was provided, and adequate food and water were available at all times.

2.2. Experimental design

The experimental design is illustrated in Fig. 1a, in which Sprague−Dawley rats were anesthetized with varying concentrations of isoflurane. As depicted in Fig. 1b [25], the MEAs was implanted into the CA1 of the rats, which was used to record the electrophysiological signals including the spike firings of the neurons and LFPs.

Three replicate experiments were performed in the presented study. The electrophysiological signal was obtained through the homemade electrophysiological recording system. The spike sampling frequency was set to 30 kHz, while the LFPs sampling frequency to 1 kHz. The physiological characteristics were characterized based on the respiratory rate, which was measured every 2 min for 30 s each time during the experiment.

2.3. Design, fabrication and modification of MEAs

In order to record the electrophysiological signals in field CA1 of the hippocampus (CA1), the MEAs were designed with 32 microelectrodes, each with a diameter of 5 μm. The microelectrodes were distributed at the tips of four 5 mm shanks, and each shank was 170 μm in width, 25 μm in thickness and 120 μm spacing to match the size of neurons and the depth, shape and size of CA1, as shown in Figs. 2a, b and S1.

The silicon-based MEAs were fabricated based on micro electromechanical system (MEMS) process described in a previous report [26]. As illustrated in Fig. 1c, the fabrication process involved the following steps: (i) The MEAs were fabricated on a silicon-on-insulator (25 μm Si/1 μm SiO_2/400 μm Si), which was first subjected to thermal oxidation to produce a substrate insulation layer, in order to insulate the metal layer from the silicon substrate. (ii) The photoresist patterning for metal tracing was generated using photolithography. (iii) Ti/Pt was sputtered to form the metal layer. (iv) The metal layer pattern was formed by lift-off. (v) SiO_2/Si_3N_4 was deposited by plasma enhanced chemical vapor deposition technique, which produced an insulation layer. (vi) The photoresist patterning for the exposed sites was conducted using photolithography. (vii) The insulation layer (SiO_2/Si_3N_4) was etched using CHF_3 reactive ion etching to expose the recording sites. (viii) The photoresist patterning for the shape of the MEAs was performed using photolithography. (ix) The SiO_2/Si layer was etched using the deep reactive ion etching technique, which formed the shape of the MEAs. (x) The MEAs were released from the wafer by wet etching.

In order to record the electrophysiological signals with high spatiotemporal resolution, it is necessary to reduce the microelectrode impedance, which was achieved using a surface modification technique. All microelectrodes (S01-S32) were modified with PtNPs by chronoamperometry (−1.17 V, 120 s) using a two-electrode system with Pt as the reference electrode.

2.4. Electrophysiological signals recording of the hippocampal CA1 using the MEAs

In the surgery, the rats were first anesthetized with isoflurane (3%–5% for induction and 0.8%–1.5% for maintenance) and then fixed in the stereotaxic frame. The hair and scalp of the rat were cut using a razor to expose the skull. The coordinates of craniotomy were 3 mm behind the midline and 1.5 mm laterally (AP: 1.5 mm, ML: 3 mm). A skull screw was fixed on the skull of the rat as the grounding electrode, and a window was formed using a skull drill at the target position on the skull. Afterward, the rats and all equipment were placed into the electromagnetic shielding box to eliminate the interference of external noise. Next, the MEAs was implanted into the rat's brain via the formed window (DV: 3 mm).

After the surgery, the shield box and the skull screw were connected with copper wires as grounding to improve the SNR of the signal. The MEAs and the homemade electrophysiological signal record-

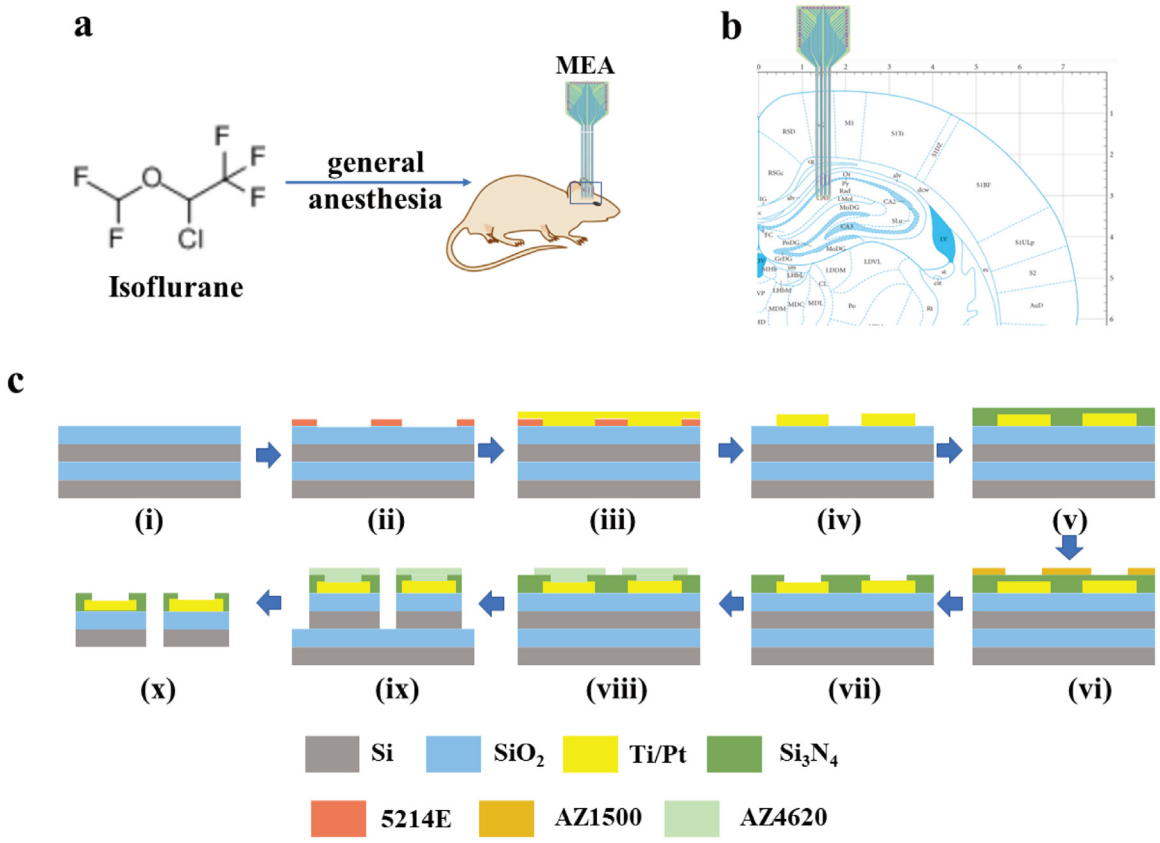

Fig. 1. The schematic diagram of experiment process technological and the process of MEAs fabrication. (a) Scheme of animal experiment, the MEAs were implanted in the brains of rats anesthetized by isoflurane. (b) Position of the MEA implantation, which is a magnified image of the blue box in (a). (c) Schematic diagram of the fabrication process of MEAs: (i) Thermal oxidation on SOI to produce a layer of SiO_2. (ii) Generate the photoresist patterning for metal trace by photolithography (5214E). (iii) Sputtering metal layer (Ti/Pt). (iv) Pattern metal layer by lift-off. (v) Deposition of SiO_2/Si_3N_4 by plasma enhanced chemical vapor deposition. (vi) Generate the photoresist patterning for exposed site by photolithography (AZ1500). (vii) Insulation layer (SiO_2/Si_3N_4) etching. (viii) Generate the photoresist patterning for shape of the MEAs by photolithography (AZ4620). (ix) SiO_2/Si layer etching. (x) Releasing of the MEAs.

ing equipment were connected with copper wires to record the electrophysiological signals. The electrophysiological signals detected by the MEAs were further processed by the amplifier and then simultaneously imported into the data acquisition module. Afterward, the signals were imported to the signal acquisition software via a universal serial bus.

2.5. Statistical analysis

The result data were presented as mean ± SD. The statistical significance was set at $P < 0.05$ (ANOVA analysis). The exact statistical method is indicated in the figure legends, 'N' always refers to the number of experiences, and 'n' always refers to the number of channels. In addition, 20 of the 32 channels with higher SNR were selected for further statistical analysis to ensure the accuracy of the results.

NeuroExplorer 4 (Nex Technologies, USA) and Offlinesorter (Plexon, USA) were used for spike classification and preliminary processing.

3. Results and discussion

3.1. Characterization of the electrical performance of microelectrodes

The microscopic image of the surface of the microelectrodes fabricated based on MEMS processing technology is shown in Fig. 2b. The microscopic image of the PtNPs-modified sites is shown in Fig. 2c. As visible in the figure, the surface of the modified sites is covered with a layer of rough black nanomaterial, indicating that the surface was successfully modified with PtNPs. The morphology of the PtNPs modified microelectrodes was characterized by scanning electron microscopy (SEM), and the SEM images are depicted in Figs. 2d and S2. As visible in the figures, PtNPs tightly adhered to the microelectrode surface, and the nanomaterial formed rich nanostructures, making the microelectrode surface rougher and increasing the surface area of the microelectrode effectively. This would improve the electrical conductivity and electrical performance of the microelectrode.

In order to characterize the electrical properties of the microelectrodes, the electrochemical impedance spectroscopy (EIS) of all 32 microelectrodes in the standard PBS was carried out based on the traditional three-electrode system to characterize the impedance and phase delay performance of the microelectrodes (Fig. 2e, f). In the frequency range from 10 Hz to 1 MHz, a significant reduction in the impedance and phase delay was observed for the modified microelectrodes compared to the bare ones, indicating that the PtNPs-modified sites present a lower impedance and phase delay.

At the frequency of 1 kHz, which is commonly used in neuroscience studies as the central frequency of neural activity [27], the impedance of the PtNPs-modified microelectrode was 11.5 ± 1 kΩ and the phase delay was −18.5° ± 2.54°, and these values had reduced from the corresponding values of 1504 ± 350 kΩ and −73.2° ± 2.89°, respectively, for the bare electrode. These results demonstrated that PtNPs modification could reduce the characteristic impedance of the microelectrode at 1 kHz to 7.64% and the phase delay to 25% compared to the corresponding values for the bare electrode, which implied that the electrical

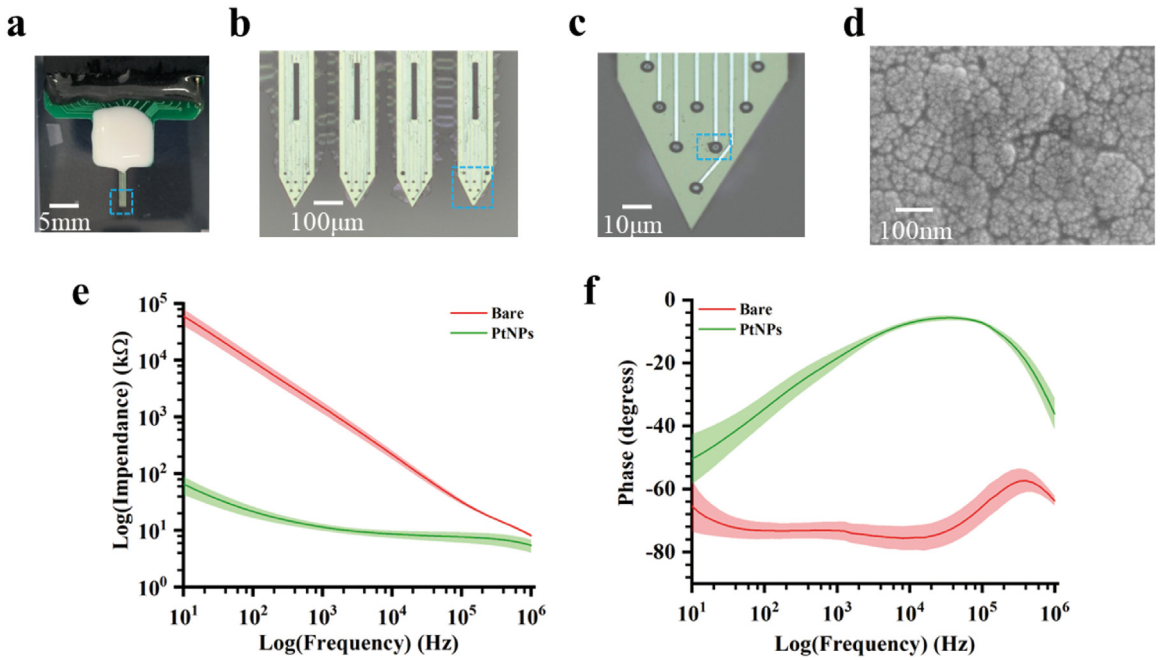

Fig. 2. PtNPs-modified MEAs and electrical performance characterization of the MEAs. (a) Completed MEAs connected with the printed circuit board. (b) 32 sites distributed on the tip of four shanks, which is a magnified image of the blue box in (a). (c) Microscopic images of the PtNPs-modified sites, which is a magnified image of the blue box in (b). (d) Morphology of the PtNPs-modified sites characterized by scanning electron microscopy, which is a magnified image of the blue box in (c). (e) Impedance characteristics of bare and PtNPs-modified sites at different frequencies. The shadow is the error bar calculated from the impedance characteristics of thirty sites. (f) Phase characteristics of bare and PtNPs-modified sites at different frequencies. The shadow is the error bar calculated from the phase characteristics of thirty sites.

performance of the microelectrode was significantly improved by PtNPs modification.

In order to characterize the electrophysiological signal recording performance of the fabricated MEAs in vivo, the MEAs were implanted into the hippocampus CA1 of rats with spikes and LFPs recorded by twelve representative channels were shown in Fig. 3a, b. It was observed that the MEAs could record the multi-channel electrophysiological signals. The detected raw signals are presented in Figs. 3c and S3. The SNR was calculated by using the formula [28]: SNR = $V/2\sigma$, where V was the peak-to-peak value of the mean spike waveform and σ was the standard deviation of the baseline noise. In general, SNR ranged from 5.5 to 13.5 in 20 representative channels, and the average SNR of 20 channels was 8.75, which was comparable to earlier research [29,30]. This indicated that the MEAs were capable of recording the electrophysiological signals accurately, which implied that the MEAs could deliver multi-channel detection functions for neuronal activity with high SNR.

The representative spikes waveforms recorded by MEAs are presented in Fig. 3d. The waveforms of the multi-unit spikes recorded by S17 are shown in Fig. 3di. According to the previous research [5,31,32], the spikes of single neurons were sorted by the following methods: first, the waveforms of multi-unit spikes were mapped into the two-dimensional plane by principal component analysis. Then, the action potential waveforms of single-unit were then separated by K-means cluster analysis (Fig.S4), The results of spike-sorting are shown in Fig. 3dii, which showed the action potential waveforms fired by three single neurons recorded by S17. In addition, more waveforms of single-unit spikes recorded by different channels are presented in Fig. S5, and the inter-spike interval histogram of single-unit spikes recorded by S17 was provided in Fig.S6, which showed that the first few bins of the histogram were empty, which indicated the spikes were fired by single-units. Therefore, it was convincing that the MEAs were capable of recording neuronal spike firing activity accurately, thus, the MEAs could detect the neural information in hippocampal CA1 at the single-cell level accurately.

3.2. Characteristics of the electrophysiological signals with varying isoflurane concentration

The dynamic processes of the electrophysiological signals in the CA1 brain region of rat hippocampus and the respiratory rate during the change in the isoflurane anesthetic concentration were further analyzed. The changes in the isoflurane anesthetic concentration over time are presented in Fig. 4a. The isoflurane anesthetic concentration increased from 1.0% to 1.75%, followed by a decrease to 1%, with a gradient of 0.25%, and each concentration maintained for 120 s. Fig. 4b presents the variations in the rat respiratory rate during the change in the isoflurane concentration. The respiratory rate decreased significantly with the increase in the isoflurane concentration and reached a minimum value of 29 times/min at 560 s. The minimum values of respiratory rate appeared within 120 s after the maximum value of isoflurane concentration and were maintained for a period of time.

The spike raster in the representative channel (S05) is shown in Fig. 4c. The average value of the spike firing rate recorded by the 20 microelectrodes was calculated (as shown in Fig. 4d). The spike firing rate was observed to decrease over time. The spike firing rate decreased from the peak value of 12 Hz at 0 s to the minimum of 0.5 Hz at 600 s, then maintained until 820 s. In addition, the variations in the spike firing rate with the isoflurane anesthetic concentration were observed, which revealed that the spike firing rate decreased with the increase of isoflurane concentration from 1% to 1.75% and then maintained even when the isoflurane concentration decreased from 1.75% to 1%. This result indicated that isoflurane could inhibit spike firing activity of neurons and isoflurane at the concentration of 1.75% caused a sustained effect on the spike firing activity of neurons.

The LFPs of the representative channel (S05) is shown in Fig. 4e, and Fig. 4f, g presents the statistical analysis results for the LFPs recorded in 20 channels. The average value of the power of LFPs was calculated (as shown in Fig. 4f). It was observed that the LFPs power increased and then maintained over time. In the 0–600 s period, there was an increase

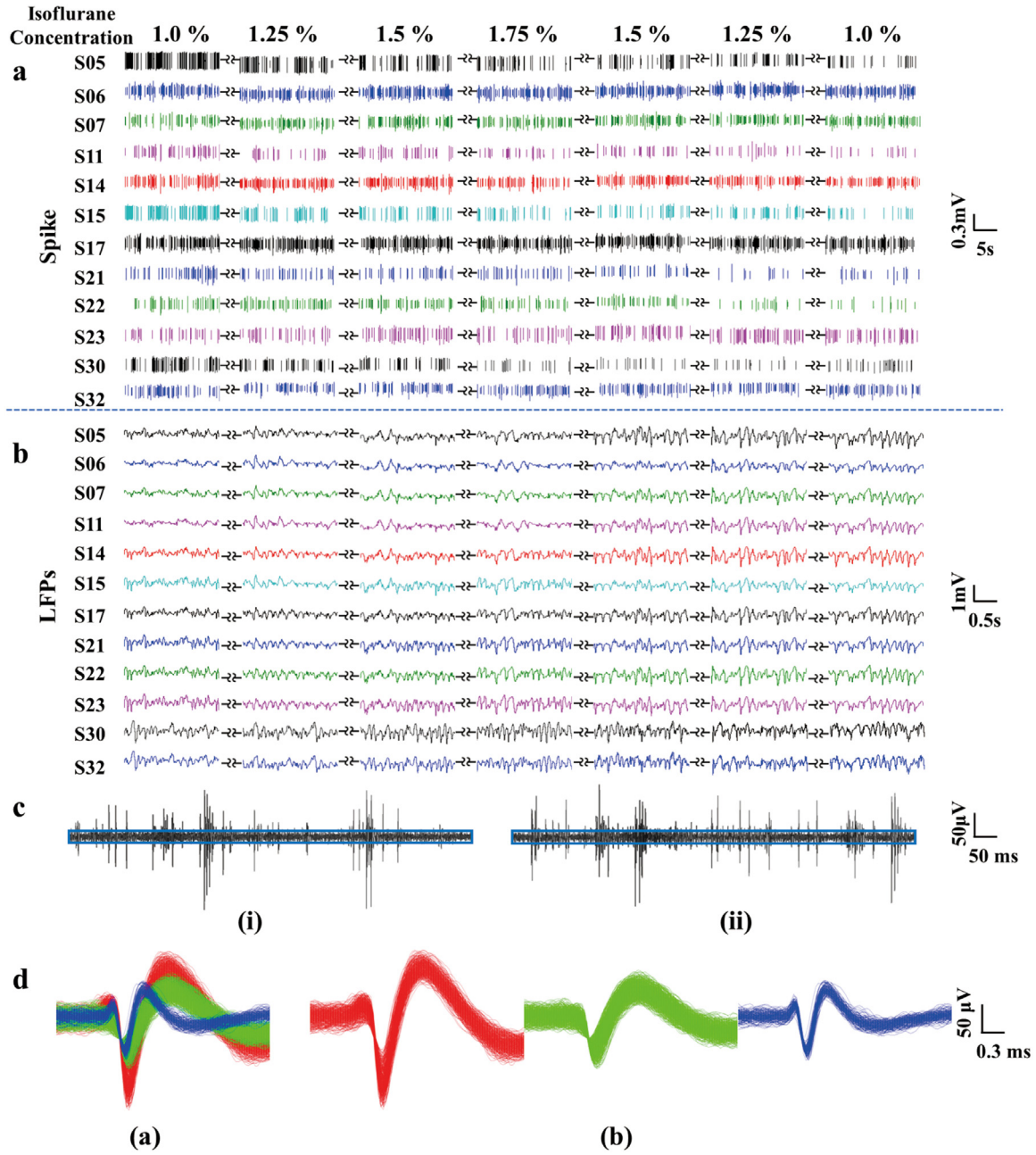

Fig. 3. Electrophysiological signals detected by the PtNPs-modified MEAs. (a) Representative twelve channels of spike raster. (b) Representative twelve channels of LFPs. (c) Raw data of electrophysiological signals recorded by S14 (i) and S17 (ii) of the MEAs, the blue box showed the baseline noise. (d) Representative spikes recorded by and S17 of the MEAs: (i) Waveforms of multi-unit spikes recorded by channel S17. (ii) Waveforms of action potentials fired by three single-unit obtained by spike sorting.

from 1.5 μW to 2.75 μW, while the power was maintained at around 2.4 μW until 820 s. When the variations in the power of LFPs with the isoflurane anesthetic concentration were observed, it was revealed that the power of LFPs increased with the increase of isoflurane concentration from 1% to 1.75% and then maintained even when the isoflurane concentration decreased from 1.75% to 1%, These results indicated that isoflurane at the concentration of 1.75% caused a sustained effect on the power of LFPs. Fig. 4g depicts the spectrograms of the LFPs. It can be observed that the total power of LFPs increased over time gradually from 0 to 600 s and then maintained over time. The power change was more evident around 8 Hz. When the variations in the spectrogram of the LFPs with the isoflurane anesthetic concentration were observed, it was revealed that the total power of LFPs increased with the increase of isoflurane concentration and the power of LFPs changed most significantly around 8 Hz.

3.3. Characteristics of spike under different concentrations of isoflurane anesthetic

Rats were subjected to different levels of anesthesia mediated by various concentrations of isoflurane. Statistical analysis was performed on the spike firing rates under different degrees of isoflurane anesthesia. The spike firing rates of hippocampal CA1 neurons were significantly different under the different concentrations of isoflurane anesthetic, as depicted in Fig. 5a. It was shown that the firing rates decreased significantly with the increase in the isoflurane concentration, and the aver-

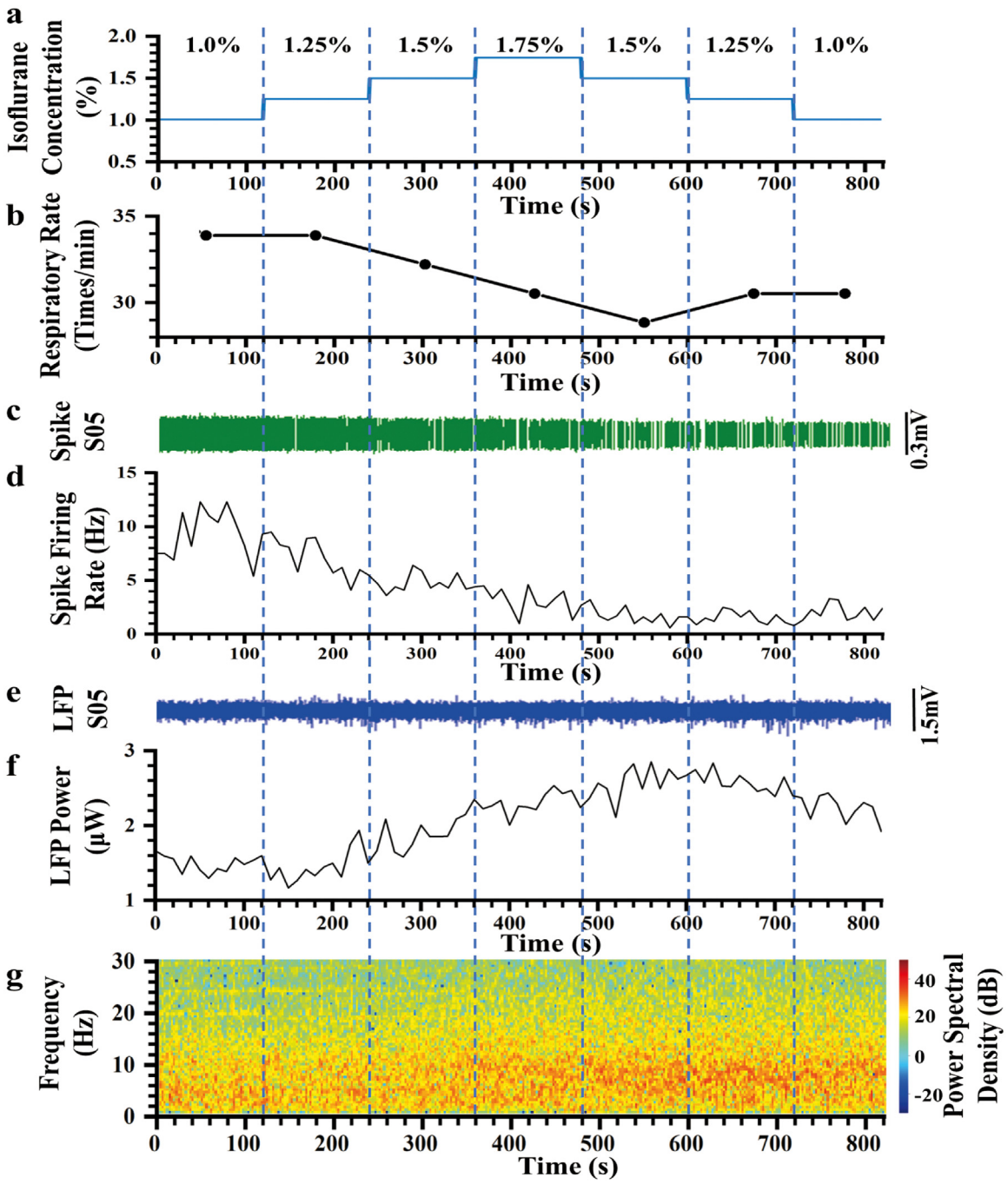

Fig. 4. Characteristics of the electrophysiological signals during changes in isoflurane concentration. (a) Variation of isoflurane concentration. (b) Dynamic variations of respiratory rate in rats under isoflurane anesthesia with varying concentrations. (c) Spike firing recorded by S05 during changes in isoflurane concentration. (d) Average spike firing rate during the change in anesthetic concentration ($N = 3$, $n = 20$). (e) LFPs recorded by S05 during changes in isoflurane concentration. (f) Average LFPs power histogram ($N = 3$, $n = 20$). (g) Spectrogram of LFPs ($N = 3$, $n = 20$).

age firing rate at 1.75% isoflurane concentration was just 54% of the average firing rate at 0.5% isoflurane concentration. The spike waveforms under different levels of isoflurane anesthesia were analyzed and compared (Fig. 5b). It was shown that the amplitude of the spike waveforms decreased with the increase of isoflurane concentration. The average spike power at different concentrations of isoflurane anesthetic was calculated and analyzed (Fig. 5c). It was shown that the average spike power under 0.5% isoflurane concentration was higher than that under 1.75% isoflurane concentration, thus, the spike power decreased with the increase of isoflurane concentration.

3.4. Characteristics of LFPs under different concentrations of isoflurane anesthesia

LFPs are a complex combination of the electrophysiological activities of several neurons around the recording microelectrode [33]. Rats were subjected to different levels of anesthesia mediated by different concentrations of isoflurane, as recorded by representative channels of the hippocampal CA1 LFPs shown in Fig. 6a. Low-frequency oscillations were observed at higher isoflurane concentrations, and the amplitude of the LFPs was also enhanced.

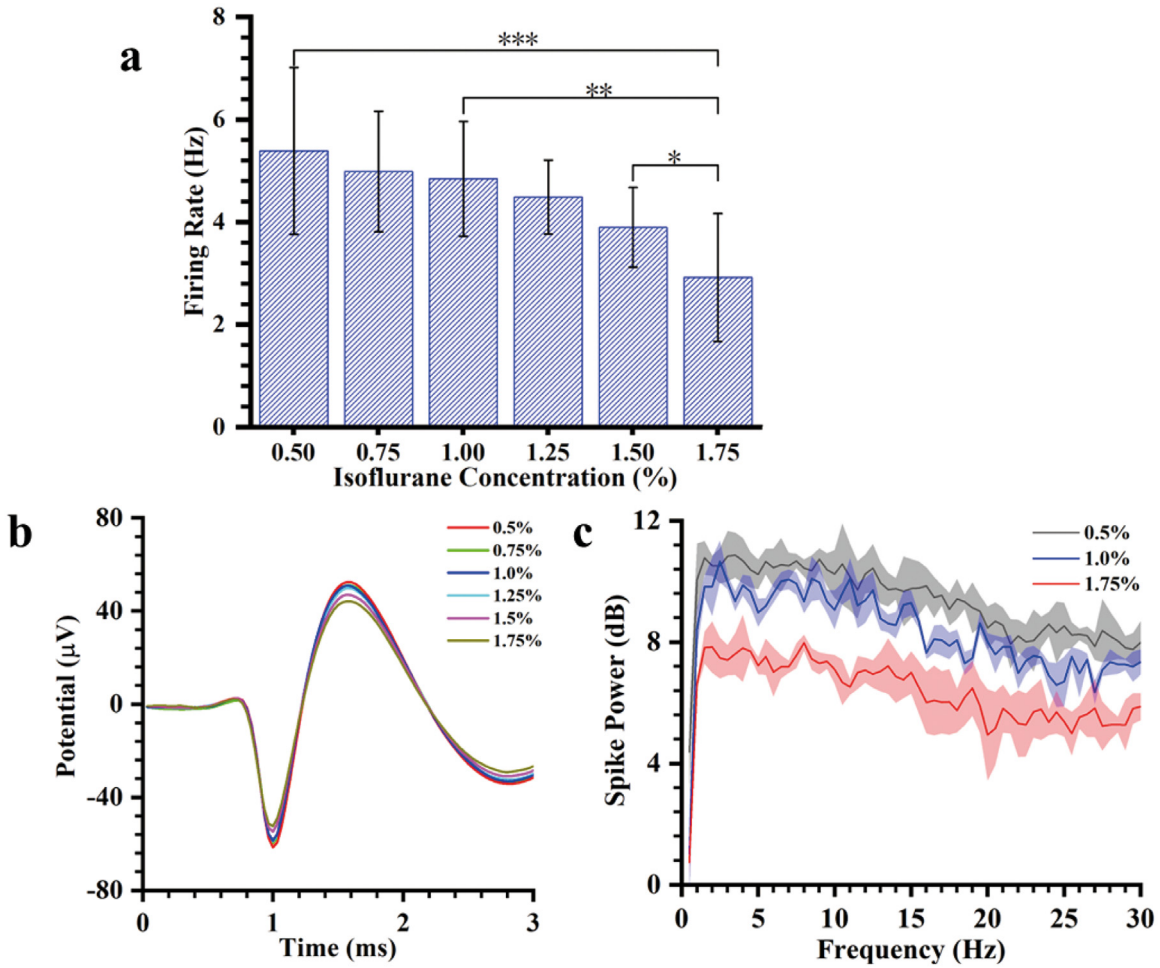

Fig. 5. Characteristics of the spikes at different concentrations of isoflurane anesthesia. (a) Statistical analysis of the average spike firing rates at different concentrations of isoflurane anesthesia ($N = 3$, $n = 20$; $^{***}P < 0.001$; $^{**}P < 0.01$; $^{*}P < 0.05$). (b) The average spike waveform of rats at different concentrations of isoflurane anesthesia ($N = 3$, $n = 20$). (c) The average spike power at different concentrations of isoflurane anesthesia ($N = 3$, $n = 20$). The shadow is the error bar calculated from the spike power of 20 channels.

The PSDs of the LFPs at different concentrations of isoflurane are shown in Fig. 6b. The total power of LFPs was enhanced with the increase of isoflurane concentration. The power around 8 Hz changed more significantly, and the peak of PSD moved from 4 Hz to 8 Hz. The LFPs were divided into four bands for power calculation based on their frequency (Fig. 6c), the power of δ band (0–4 Hz) was maintained while the power of α (7–13 Hz), β (13–30 Hz), and θ (4–7 Hz) bands enhanced with the increase of isoflurane concentration. Among these, the power enhancements of α and θ bands were more obvious, which was consistent with the phenomenon presented in Fig. 6b. The spectrograms of the LFPs under different concentrations of isoflurane are shown in Fig. 6d. It was observed that the power of LFPs was lowest at 0.5% isoflurane concentration, enhanced at 1% isoflurane concentration, and significantly increased at 1.75% isoflurane concentration. Furthermore, the power enhancement of the LFPs around 8 Hz was more significant. This phenomenon was consistent with the results of previous research [34,35], which reported that inhaled anesthetics such as isoflurane could enhance low-frequency oscillations and increase the amplitude and power of oscillations in the brain to maintain the anesthesia.

3.5. Correlation between electrophysiological signals and anesthetic concentration

The accurate recording of neuron electrophysiological signals from the deep brain is an important topic in neuroscience. MEAs, as a minimally invasive signal detection tool, have great advantages in the detection of electrophysiological signals from the deep brain [36–38]. Owing to their micron-level sizes, MEAs cause little damage to the brain tissue and have almost no effect on experimental results. In addition, MEAs have a high spatial and temporal resolution, allowing real-time accurate detection of the electrophysiological activity of individual neurons [31]. The modification of PtNPs substantially reduced the impedance and phase delay of the microelectrodes by increasing the contact area between the surface of the microelectrodes and the neurons, thus improving the electrical performance of MEAs and facilitating the accurate detection of neural activity.

Isoflurane anesthetic exerts a wide range of influence on the brain, and the hippocampus is an important part of the anesthesia-wake neural circuit. Therefore, further study on the electrophysiological and electrochemical signals under the influence of isoflurane in this area would contribute to an in-depth understanding of the mechanism of isoflurane anesthetic and provide research methods and technical means for the monitoring of clinical anesthesia. In recent years, a series of studies have been conducted to demonstrate that isoflurane affects neural activity in hippocampal CA1, causing changes in EEG, LFPs, and leading to anesthetic-induced amnesia [39]. These findings drove the present investigation on neuronal activity in hippocampal CA1 under isoflurane anesthesia, therefore the isoflurane anesthesia model was selected to detect the neuron electrophysiological signals in hippocampal CA1.

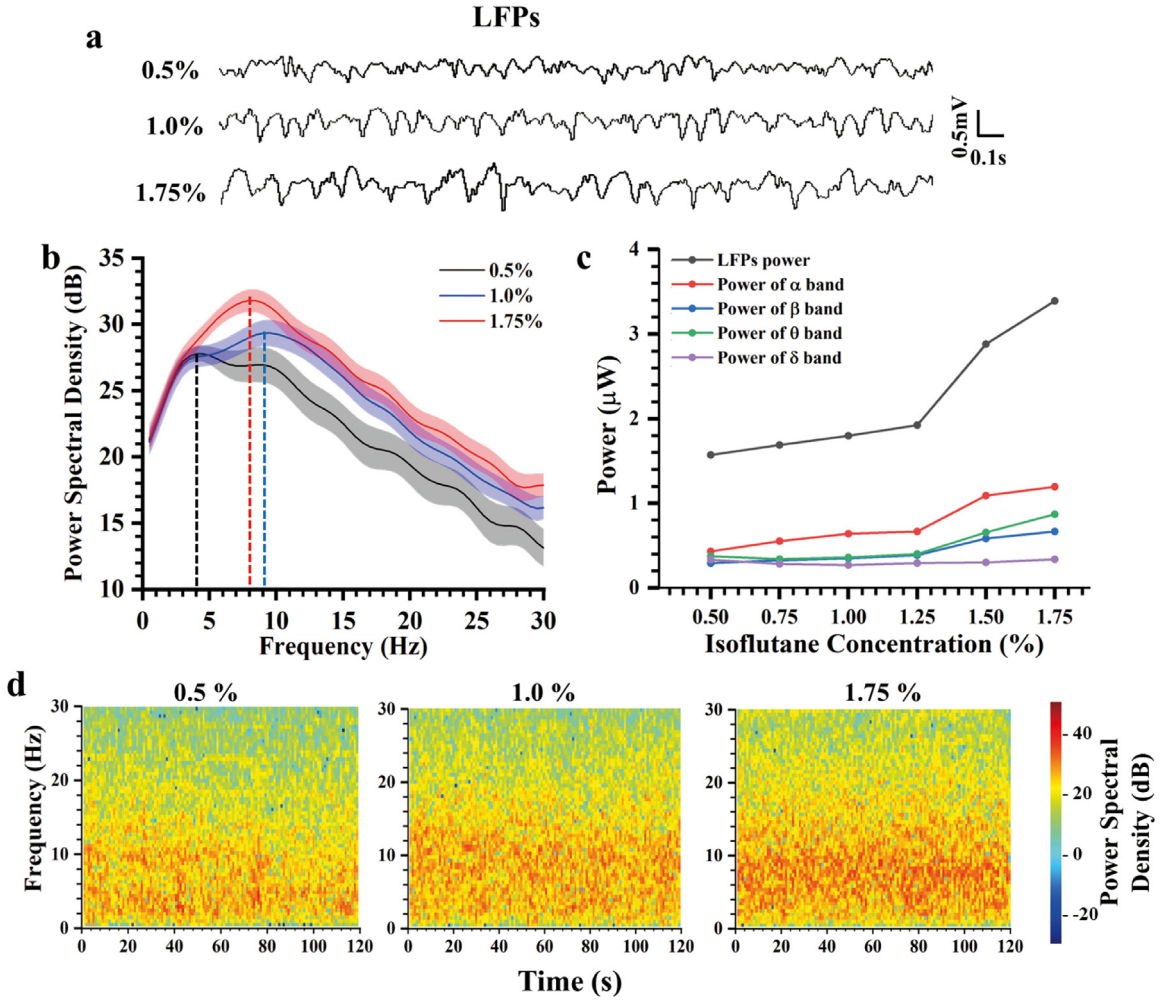

Fig. 6. Characteristics of the LFPs at different concentrations of isoflurane anesthesia. (a) Representative channels of LFPs at different concentrations of isoflurane anesthesia. (b) Power spectral density (PSD) of LFPs at different concentrations of isoflurane anesthesia in the frequency band of 0–30 Hz. The shadow is the error bar calculated from the PSD of the LFPs recorded by sixteen channels ($N = 3$, $n = 20$). (c) Power of LFPs and different frequency oscillation at different concentrations of isoflurane anesthesia ($N = 3$, $n = 20$). (d) Spectrogram of LFPs at different concentrations of isoflurane anesthesia ($N = 3$, $n = 20$).

With changes in isoflurane concentration, significant changes were recorded in the hippocampal CA1 region of rats (Fig. 4), in terms of both physiological characteristics and neuron electrophysiological signals (spike and LFPs). The respiratory rate and the spike firing rate were observed to decrease with increasing isoflurane concentration, while the power of LFPs increased with increasing isoflurane concentration. A strong correlation existed between such changes and the variations in isoflurane concentration, indicating that hippocampal CA1 neurons are sensitive to isoflurane concentration. Further, when the isoflurane concentration was gradually decreased from 1.75% to 1.0%, the spike firing rate and LFPs power were maintained for a period of time, indicating a sustained effect of isoflurane on the neurons in CA1. These findings suggested that the activity of CA1 neurons in the rat hippocampus could reflect changes in isoflurane concentration in real time and could be used to characterize the degree of anesthesia.

Electrophysiological signals in rat hippocampal CA1 showed significant differences among different levels of isoflurane-mediated anesthesia at different isoflurane concentrations. CA1 spike firing activity varied with the degrees of anesthesia (Fig. 5). The spike firing rate of lower concentration isoflurane was significantly higher than that of higher concentrations, the amplitude of spikes at lower concentration isoflurane was slightly increased compared to that of higher concentrations, and the spike power at lower concentrations of isoflurane was slightly enhanced compared to that of higher concentrations. These results indicated that isoflurane could inhibit the spike-firing activity of CA1 neurons. CA1 LFPs varied with the different degrees of anesthesia (Fig. 6). The LFPs exhibited slow-wave oscillation characteristics at higher concentrations of isoflurane, which induced the enhancement of low-frequency power in LFPs. The power of the LFPs at low concentrations of isoflurane was lower than that at high concentrations, furthermore, the power change was most obvious around 8 Hz. These results were consistent with the results of previous research, which reported that the amplitude and power of oscillations in the brain increased during anesthesia procedure [34,35]. We propose that the reason for this phenomenon in LFPs is that isoflurane induces and enhances low-frequency oscillations in the CA1 region of the hippocampus and causes slow-wave phenomena in the LFPs. Consequently, the amplitude and power of LFPs increase under isoflurane anesthesia [40–42]. This phenomenon is inconsistent with changes in the spike firing activity, which may be explained by the fact that neurons do not fire action potentials does not imply that they have no potentiation activity; its membrane potential continues to receive excitatory or inhibitory postsynaptic potential information as well as generates potential fluctuations within a certain range, and this subthreshold neural potential activity constitutes the main source of the formation of LFPs [43,44]. These phenomena suggest that both electrophysiological signals in rat hippocampal CA1 are capable of characterizing different concentrations of isoflurane anesthetic and could be used for monitoring the level of isoflurane anesthesia.

4. Conclusion

Four-shank 32-channel implantable MEAs were designed and fabricated for detecting electrophysiological signals in the hippocampal CA1 during anesthesia with varying concentrations of isoflurane. In order to improve the electrical performance of the MEAs, the microelectrode surface was modified with PtNPs to detect the electrophysiological signals at low impedance (11.5 ± 1 kΩ), small phase delay (−18.5° ± 2.54°) and high SNR (8.75). In this way, we could detect neural information in hippocampal CA1 at the single-cell level with high spatial and temporal resolution.

The signals detected by MEAs revealed that isoflurane can affect neuronal activities in the rat hippocampus. Isoflurane anesthesia was capable of inhibiting the spike-firing activity of neurons in hippocampal CA1 and enhancing low-frequency oscillations in CA1, resulting in the increase of low-frequency power in LFPs. In addition, higher concentrations (1.75%) of isoflurane were capable of causing sustained effects on neuronal activity in hippocampal CA1. These phenomena suggest that the spike firing activity of CA1 neurons and LFPs power of CA1 could reflect the isoflurane concentration during the isoflurane anesthesia procedure.

The utilization of detecting MEAs allowed for the exploration of the dynamic procedure of isoflurane anesthesia at the single-cell level in hippocampal CA1, and provided a research method for the monitoring of clinical anesthesia. Anesthetics have a wide range of effects on the neuronal activities in the brain. Our research only detected and analyzed the neural information of hippocampal CA1 during anesthesia, more relevant nuclei need to be studied in depth in subsequent work. During clinical general anesthesia, several different anesthetics are used simultaneously. In our study, only the effects of isoflurane were explored, and the effects of more commonly used anesthetics need to be investigated in subsequent work. The implantation of MEAs was minimally invasive, and non-invasive methods are more necessary for clinical anesthesia monitoring. If we can correlate the EEG and electrophysiological signal characteristics and discover the characteristics of EEG under isoflurane anesthesia, it will support to develop an accurate technology to monitor anesthesia degrees.

Declaration of competing interest

The authors declare that they have no conflicts of interest in this work.

Acknowledgments

This work was sponsored by the National Natural Science Foundation of China (T2293731, 61960206012, 62121003, 62171434, 61971400, 61975206, and 61973292); the Scientific Instrument Developing Project of the Chinese Academy of Sciences (GJJSTD20210004); the National Key Research and Development Program (2022YFC2402501, 2022YFB3205602); Major Program of Scientific and Technical Innovation 2030 (2021ZD0201603).

Supplementary materials

Supplementary material associated with this article can be found, in the online version, at doi:10.1016/j.fmre.2023.05.015.

References

[1] V. Sorrenti, C. Cecchetto, M. Maschietto, et al., Understanding the effects of anesthesia on cortical electrophysiological recordings: A scoping review, Int. J. Mol. Sci. 22 (3) (2021) 1286.
[2] E.I. Eger, The pharmacology of isoflurane, Br. J. Anaesth. 56 (1) (1984) S71–S99.
[3] M.R. Shaughnessy, E.H. Hofmeister, A systematic review of sevoflurane and isoflurane minimum alveolar concentration in domestic cats, Vet. Anaesth. Analg. 41 (1) (2014) 1–13.
[4] X.R. Li, Y.L. Song, G.H. Xiao, et al., Flexible electrocorticography electrode array for epileptiform electrical activity recording under glutamate and gaba modulation on the primary somatosensory cortex of rats, Micromachines 11 (8) (2020) 732.
[5] K. Purtelll, K.J. Gingrich, W. Ouyang, et al., Activity-dependent depression of neuronal sodium channels by the general anaesthetic isoflurane, Br. J. Anaesth. 115 (1) (2015) 112–121.
[6] W. Ouyang, G. Wang, H.C. Hemmings, Isoflurane and propofol inhibit voltage-gated sodium channels in isolated rat neurohypophysial nerve terminals, Mol. Pharmacol. 64 (2) (2003) 373–381.
[7] M. Perouansky, H.C. Hemmings, Neurotoxicity of general anesthetics cause for concern? Anesthesiology 111 (6) (2009) 1365–1371.
[8] L.S. Leung, T. Luo, J.Y. Ma, et al., Brain areas that influence general anesthesia, Prog. Neurobiol. 122 (2014) 24–44.
[9] L. Uhrig, S. Dehaene, B. Jarraya, Cerebral mechanisms of general anesthesia, Ann. Fr. Anesth. Reanim. 33 (2) (2014) 72–82.
[10] B.S. Chortkoff, H.L. Bennett, E.I. Eger, Subanesthetic concentrations of isoflurane suppress learning as defined by the category-example task, Anesthesiology 79 (1) (1993) 16–22.
[11] M. Perouansky, V. Rau, T. Ford, et al., Slowing of the hippocampal theta rhythm correlates with anesthetic-induced amnesia, Anesthesiology 113 (6) (2010) 1299–1309.
[12] H.C. Hemmings, M.H. Akabas, P.A. Goldstein, et al., Emerging molecular mechanisms of general anesthetic action, Trends Pharmacol. Sci. 26 (10) (2005) 503–510.
[13] B. Antkowiak, Molecular and neuronal substrates for general anaesthetics, Acta Physiol 210 (2014) 22-22.
[14] N.P. Franks, Molecular targets underlying general anaesthesia, Br. J. Pharmacol. 147 (2006) S72–S81.
[15] X.S. Zhang, R.J. Roy, E.W. Jensen, EEG complexity as a measure of depth of anesthesia for patients, IEEE Trans. Biomed. Eng. 48 (12) (2001) 1424–1433.
[16] L.M. Antunes, H.D. Golledge, J.V. Roughan, et al., Comparison of electroencephalogram activity and auditory evoked responses during isoflurane and halothane anaesthesia in the rat, Vet. Anaesth. Analg. 30 (1) (2003) 15–23.
[17] O. Akeju, M.B. Westover, K.J. Pavone, et al., Effects of sevoflurane and propofol on frontal electroencephalogram power and coherence, Anesthesiology 121 (5) (2014) 990–998.
[18] J.A. Guidera, N.E. Taylor, J.T. Lee, et al., Sevoflurane induces coherent slow-delta oscillations in rats, Front. Neural Circ. 11 (2017) 36.
[19] G.H. Xiao, Y.L. Song, Y. Zhang, et al., Microelectrode arrays modified with nanocomposites for monitoring dopamine and spike firings under deep brain stimulation in rat models of Parkinson's disease, ACS Sens. 4 (8) (2019) 1992–2000.
[20] M.D. Johnson, R.K. Franklin, M.D. Gibson, et al., Implantable microelectrode arrays for simultaneous electrophysiological and neurochemical recordings, J. Neurosci. Meth. 174 (1) (2008) 62–70.
[21] E.H. He, S.W. Xu, Y.C. Dai, et al., Swcnts/Pedot:PSS-modified microelectrode arrays for dual-mode detection of electrophysiological signals and dopamine concentration in the striatum under isoflurane anesthesia, ACS Sens. 6 (9) (2021) 3377–3386.
[22] H. Jan, R. Gul, A. Andleeb, et al., A detailed review on biosynthesis of platinum nanoparticles (Ptnps), their potential antimicrobial and biomedical applications, J. Saudi Chem. Soc. 25 (8) (2021) 101297.
[23] S.W. Xu, L. Wang, X.T. Song, et al., Synchronous detection of rat neural spike firing and neurochemical signals based on dual-mode recording instrument, Chinese J. Anal. Chem. 44 (9) (2016) 1457–1463.
[24] S.W. Xu, Y. Zhang, S. Zhang, et al., An integrated system for synchronous detection of neuron spikes and dopamine activities in the striatum of Parkinson monkey brain, J. Neurosci. Meth. 304 (2018) 83–91.
[25] G. Paxinos, C. Watson, Rat Brain in Stereotaxic Coordinates, 4th Ed., 1998.
[26] X.Y. Fan, Y.L. Song, Y.L. Ma, et al., In situ real-time monitoring of glutamate and electrophysiology from cortex to hippocampus in mice based on a microelectrode array, Sensors 17 (1) (2017) 61.
[27] A. Prasad, J.C. Sanchez, Quantifying long-term microelectrode array functionality using chronic in vivo impedance testing, J. Neural. Eng. 9 (2) (2012) 026028.
[28] S. Suner, M.R. Fellows, C. Vargas-Irwin, et al., Reliability of signals from a chronically implanted, silicon-based electrode array in non-human primate primary motor cortex, IEEE Trans. Neural Syst. Rehabil. 13 (4) (2005) 524–541.
[29] A. Prasad, Q.-S. Xue, R. Dieme, et al., Abiotic-biotic characterization of Pt/Ir microelectrode arrays in chronic implants, Front. Neuroeng. 7 (2014) 2.
[30] J.W. Jang, Y.N. Kang, H.W. Seo, et al., Long-term in-vivo recording performance of flexible penetrating microelectrode arrays, J. Neural. Eng. 18 (6) (2021) 066018.
[31] Y.C. Dai, Y.L. Song, J.Y. Xie, et al., Cb1-Antibody modified liposomes for targeted modulation of epileptiform activities synchronously detected by microelectrode arrays, ACS Appl. Mater. Interfaces. 12 (37) (2020) 41148–41156.
[32] J. Csicsvari, H. Hirase, A. Czurko, et al., Reliability and state dependence of pyramidal cell-interneuron synapses in the hippocampus: An ensemble approach in the behaving rat, Neuron 21 (1) (1998) 179–189.
[33] G. Buzsaki, C.A. Anastassiou, C. Koch, The origin of extracellular fields and currents - Eeg, Ecog, Lfp and Spikes, Nat. Rev. Neurosci. 13 (6) (2012) 407–420.
[34] L.L. Han, S. Zhao, F. Xu, et al., Sevoflurane increases hippocampal theta oscillations and impairs memory via task-3 channels, Front. Pharmacol. 12 (2021) 728300.
[35] O. Akeju, A.E. Hamilos, A.H. Song, et al., Gabaa circuit mechanisms are associated with ether anesthesia-induced unconsciousness, Clin. Neurophysiol. 127 (6) (2016) 2472–2481.
[36] A. Zhang, E.T. Mandeville, L. Xu, et al., Ultra-flexible endovascular probes for brain recording through micron-scale vasculature, bioRxiv. (2023) 10.1101/2023.03.20.533576.

[37] Z.T. Zhao, H.L. Zhu, X. Li, et al., Ultraflexible electrode arrays for months-long high-density electrophysiological mapping of thousands of neurons in rodents, Nat. Biomed. Eng. 7 (2023) 520–532.
[38] F. He, Y.C. Sun, Y.F. Jin, et al., Longitudinal neural and vascular recovery following ultraflexible neural electrode implantation in aged mice, Biomaterials 291 (2022) 121905.
[39] R.C. Dutton, A.J. Maurer, J.M. Sonner, et al., The concentration of isoflurane required to suppress learning depends on the type of learning, Anesthesiology 94 (3) (2001) 514–519.
[40] B. Lustig, Y.X. Wang, E. Pastalkova, Oscillatory patterns in hippocampus under light and deep isoflurane anesthesia closely mirror prominent brain states in awake animals, Hippocampus 26 (1) (2016) 102–109.
[41] D. Pal, B.H. Silverstein, L. Sharba, et al., Propofol, sevoflurane, and ketamine induce a reversible increase in delta-gamma and theta-gamma phase-amplitude coupling in frontal cortex of rat, Front. Syst. Neurosci. 11 (2017) 41.
[42] D. Wang, Y.X. Guo, H.M. Li, et al., Selective optogenetic activation of orexinergic terminals in the basal forebrain and locus coeruleus promotes emergence from isoflurane anaesthesia in rats, Br. J. Anaesth. 126 (1) (2021) 279–292.
[43] A.K. Kreiter, A. Aertsen, G.L. Gerstein, A low-cost single-board solution for real-time, unsupervised waveform classification of multineuron recordings, J. Neurosci. Meth. 30 (1) (1989) 59–69.
[44] C.M. Gray, P.E. Maldonado, M. Wilson, et al., Tetrodes markedly improve the reliability and yield of multiple single-unit isolation from multi-unit recordings in cat striate cortex, J. Neurosci. Meth. 63 (1–2) (1995) 43–54.

Author profile

Ruilin Hu received her bachclor's degree of science in engineering at University of Chinese Academy of Sciences in 2020. She is currently pursuing a master's degree in State Key Laboratory of Transducer Technology, Aerospace Information Research Institute. Her research interests mainly focus on neural signal detection based on implantable microelectrode arrays.

Ying Wang received her master degree of anesthesiology at Shanghai Jiao Tong University in 2009, and became an associate chief of Anesthesiology Department at Ruijin Hospital in 2021. Since 2000 she has been engaged in clinical anesthesia work. She went to Queen Elizabeth Hospital Birmingham and Auckland University Hospital for further education in 2003 and 2008, respectively. Currently, her research mainly focuses on neural mechanisms of anesthesia and the modulation of anesthesia state.

Jinping Luo (BRID: 09833.00.15682) received her Ph.D. degree in 2008 at Institute of Electronics, Chinese Academy of Sciences, and then joined in the Brain-computer interface and micro-nano biosensor group led by Prof. Xinxia Cai in the State Key Laboratory of Transducer Technology. She became an associate professor in 2014 and accepted the key research position of the Chinese Academy of Sciences in 2022. Currently, her research mainly focuses on neural information detection and control technology based on microelectrode array.

Xinxia Cai received her Ph.D. degree at University of Glasgow in 2001. She is distinguished professor of the Aerospace Information Research Institute of the Chinese Academy of Sciences, winner of the National Science Fund for Distinguished Young Scholars, academic leader of the Micro-nano Sensing Technology Innovation Research Group of National Natural Science Foundation of China (NSFC). Prof. Cai mainly focuses on micro-nano biosensors and microsystems such as brain-computer interface neural microelectrode arrays for a long time, and is the research leader of the major project of the Interdisciplinary Department of NSFC.